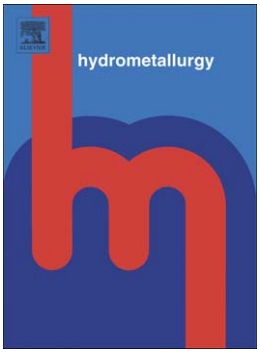

Total dissolved solids and their effects on iron oxidation by chemolithotrophic cells

K.R. Blight, R.M. Candy, M.J.M. Menzel, D.E. Ralph

PII: S0304-386X(12)00130-2
DOI: doi: 10.1016/j.hydromet.2012.05.014
Reference: HYDROM 3552

To appear in: *Hydrometallurgy*

Received date: 3 April 2012
Revised date: 23 May 2012
Accepted date: 23 May 2012

Please cite this article as: Blight, K.R., Candy, R.M., Menzel, M.J.M., Ralph, D.E., Total dissolved solids and their effects on iron oxidation by chemolithotrophic cells, *Hydrometallurgy* (2012), doi: 10.1016/j.hydromet.2012.05.014

Total Dissolved Solids and their Effects on Iron oxidation by Chemolithotrophic Cells

K.R. Blight, R.M. Candy, M.J.M. Menzel and D.E. Ralph

A.J. Parker Cooperative Research Centre for Integrated Hydrometallurgy Solutions, School of Chemical and Mathematical Sciences, Murdoch University, South Street, Murdoch, Western Australia 6150, Australia.

Abstract

Continuous growth of an acidophilic, chemolithotrophic bacterial culture in minimal iron media, was investigated over a range of TDS values. The specific cell parameters, iron oxidation rates, growth rates and observed yields at fixed solution potentials were compared over a range of TDS values but with the same total iron concentrations. By perturbing the steady state at any set point it was possible to estimate the population of sessile cells and calculate values for the specific cell parameters. The TDS was increased by addition of Na_2SO_4 which produced no toxic effects and allowed a flourishing culture. There was however significant inhibition of the specific iron oxidation rates which were reduced by more than 75% by the increase in TDS from 0.05 to 0.4 M. A framework for understanding the observed result, based on the ionic strength (*I*) rather than TDS, is suggested. The oxidation of iron is an important sub-process in hydrometallurgy and TDS values of 0.4 M are modest from an operational perspective so these results may point to potential problems during long term operation where TDS can accumulate without otherwise interfering.

Keywords: Iron oxidation, Chemolithotrophic bacteria, Inhibition, Total dissolved solids.

1.0 Introduction

Hydrometallurgical processes are concerned with iron chemistry because of the ubiquitous distribution of iron in minerals. Some control over the presence, concentration and oxidation state of iron is almost always required at some point in a process flow sheet. The oxidation of iron is the most important step in that control because the ferric state (Fe^{+3}) is the immediate precursor to forming solid iron phases which allow for its removal from the process circuit. It is often a problematic step because although reaction 1 is spontaneous, the rate is slow and becomes slower as the solution becomes more acidic (Lowson, 1982). The Fe^{+3} state is also required for the oxidation of some minerals where the target metal (M) is released as the solid is oxidatively dissolved (Eq. 2). The iron Fe^{+3}/Fe^{+2} couple in these cases

acts as a mediator, exchanging electrons between the mineral and the ultimate electron acceptor, atmospheric oxygen.

$$Fe^{+2} + H^{+} + \tfrac{1}{4}O_2 \rightarrow Fe^{+3} + \tfrac{1}{2}H_2O \quad .1$$

$$MS + 8Fe^{+3} + 4H_2O \rightarrow M^{+2} + SO_4^{-2} + 8Fe^{+2} + 8H^{+} \quad .2$$

The ferrous state (Fe^{+2}) occurs in leachate solutions by the reduction of Fe^{+3} coupled with the oxidation of a sulfide mineral (2) while the reductive leaching of ores containing iron oxides also leads to Fe^{+2} in the process solution (Hallberg et al., 2011; du Plessis et al., 2011; Bridge and Johnson 1998, 2000; Brock and Gustafson, 1976).

Rapid oxidation of Fe^{+2} can be achieved by raising the pH or by addition of oxidising agents, peroxide (H_2O_2) for example. Raising the temperature of the process solution also increases the rate of reaction 1. It's also possible to catalyse reaction 1 by the growth of chemolithotrophic cells which can be achieved by providing the solution with small amounts of salts of the 'nutrient' elements N, P, K, *etc*.. Indeed it is almost impossible to exclude these ubiquitous cells from any process circuit provided the temperature remains below the boiling point of water. Extremes of pH do not exclude the growth of these cells and strains can function over the pH range below 2.5.

While these cells will be present, any increase in rate of reaction 1 that they can provide depends, in part, on the dissolved contents of the process circuit, the medium in which the

bacteria have to grow. The effects of chloride on the bio-oxidation of Fe^{+2} have been well documented (Lawson et al., 1995; Shiers et al., 2005; Gahan et al., 2010) as have the general inhibitive effect of anions and weak organic acids (Alexander et al., 1987). Sulfate appears to be the only anion tolerated by iron oxidising cells but there are reports that even this anion has inhibitory effects at high concentration (Blight and Ralph, 2004; Candy et al., 2009; Kazadi and Petersen, 2008; Merunae et al., 2002; Sundkvist et al., 2007). The effects of total dissolved solids (TDS) on iron oxidation and cell growth have been difficult to determine quantitatively and no satisfactory framework is available to interpret experimental data. None of the published quantitative models of iron oxidation include TDS as a parameter in the rate equation (Nemati et al., 1998, Ojumu et al., 2006). This study was focussed on the relationship between TDS and the rate at which chemolithotrophic bacteria can oxidise Fe^{+2} to the Fe^{+3} state. Some models of solution chemistry (Glasstone and Lewis, 1964) and the current understanding of the structure of the iron oxidation pathway (Quatrini et al., 2009) are used to provide and understanding of the observed effects.

2. Materials and Methods

All chemicals used in this study were analytical grade reagents (AR) unless otherwise stated and all solutions were prepared with water distilled from a glass still. The chemolithotrophic organism culture used in previous studies (Blight and Ralph, 2004; 2008; Shiers et al., 2005; Candy et al., 2009) and maintained by serial transfer was used as the inoculum for the first experiment. Thereafter each new experiment was inoculated from the planktonic cells from the previous one. A pH meter (Metrohm model No. 691) and glass membrane electrode (TPS No. 1211207) were used to measure pH and calibrated using pH 1.68 and 3.65 buffers (Burkin, 2001). Temperature correction was used in all calibration and measurement procedures. Cell counts were performed using a Hauser hemocytometer with a grid area of

2.5×10^{-3} mm^2 and a volume of 2.5×10^{-10} L and using a Coulter counter (MS4) equipped with a 30 μm aperture counting a volume of 5×10^{-5} L with each determination. A platinum-metal and a reference electrode (Ag/AgCl) were used to measure the redox potential in solution. The potential of the Ag/AgCl reference electrodes with respect to a normal hydrogen electrode (*nhe*, +204 mV) was used to convert potential measurements to the *nhe* scale (E). Estimates of the ionic strength (*I*) of each medium were determined using a vapour pressure osmometer (Dampfdruk, Knauer 1974) to compare the media vapour pressures with a set of KCl standards (0 - 0.65 *m*). The activity coefficients published by Lide et al., (2005), were recalculated for 35°C then used to express molal concentrations as *I* values. An aliquot of each medium was titrated with H_2O_2 and samples were removed at different E values. These were then injected into the osmometer and *I* values determined at 35 °C (Table 1).

2.1 Growth Media

Three component solutions were prepared in bulk and used to produce a minimal growth media as required. Solution A, a sulfuric acid solution was prepared by adding concentrated AR grade H_2SO_4 to distilled water until a pH of 1.50 ± 0.05 was obtained. Solution B, a macro-nutrient solution was prepared from the following salts, $(NH_4)_2SO_4$ (5.00 g), K_2HPO_4 (2.50 g), $MgSO_4.7H_2O$ (2.50 g) and $CaCl_2.0.5H_2O$ (0.100 g) dissolved in 1.00 L of deionised water and adjusted to pH 1.50 ± 0.05 with concentrated H_2SO_4. Solution C, a solution of micro-nutrients was prepared from the following salts, $CoSO_4.7H_2O$ (2.49 g), $CuSO_4.7H_2O$ (2.81 g), $MnSO_4.H_2O$ (1.69 g), $(NH_4)_6Mo_7O_{24}.4H_2O$ (1.77 g), $NiSO_4.6H_2O$ (2.62 g) and $ZnSO_4.7H_2O$ (2.87 g) dissolved in 1.00 L of deionised water and adjusted to pH 1.50 ± 0.05 with concentrated H_2SO_4.

Minimal medium (IEM) was prepared by dissolving AR grade ferrous sulfate heptahydrate (20.00 g) in the sulfuric acid solution A. Macronutrient solution B (100 mL) and micronutrient solution C (1.0 mL) were added and the solution diluted to ca. 990 mL with sulphuric acid solution A. The pH of this solution was adjusted with concentrated H_2SO_4 to pH 1.60 ± 0.05 and diluted to 1.00 L with sulfuric acid solution A. The alternate minimal media (IEM10, IEM20, IEM40 and IEM60) were prepared in the same manner except for the inclusion of 10, 20, 40 and 60.00 g of AR grade sodium sulfate respectively with the solid ferrous sulfate. All media were filtered though 0.45 μm membranes before use. The density of each medium was measured using a pycnometer (25.0 mL). TDS values for each medium were estimated from the known mass of the solid components, excluding the waters of hydration but without including of the mass of concentrated H_2SO_4 required to adjust the initial pH.

2.2 The Reactor System

The reactor was a jacketed glass vessel with an air-tight lid and a side-arm allowing gravity overflow. Agitation was provided by a Teflon-coated magnet (3 cm) maintaining the solution in the turbulent regime. The lid had air-tight ports for a temperature thermocouple, medium inlet, platinum and reference electrodes, sub-surface air inlet and exhaust via a vertical condenser. The fixed position of the overflow dictated a quiescent volume of 275 mL while imposition of the air flow (100 mL min^{-1}) and turbulent regime gave a working volume of 235 mL at 35 °C. The surface area of the reactor exposed to medium was estimated to be 165 cm^2. Evaporative losses from the reactor after installation of the condenser (at 15 °C) were insignificant. The medium was introduced into the reactor in small aliquots using either gravity feed from a reservoir on an electronic balance or a Metrohm 775 titrator pump.

During start-up, fresh medium in the reactor was brought to temperature and inoculated. Cellular activity in the reactor increased the solution redox potential (E). At short intervals (ca 1 min) the value of E was compared to the desired set point and an aliquot of fresh medium added if E was greater (Datataker model DT50). The typical oscillations produced in this mode of operation are shown in figure 1.

2.3 Calculating culture parameters

With a constant flow rate of fresh medium characterising a particular set point, the rate of iron oxidation in the reactor was found from the volumetric flow rate (dV_m/dt) or the mass flow rates and the medium density ($dM/dt/\rho$). The difference in Fe^{+2} concentration between the reservoir and reactor fluids (Δ_{Fe+2}) was found from the respective E values (Shiers et al., 2005). The rate of iron oxidation in the reactor was then R_{Fe+2} (mol h^{-1}) = $-\Delta_{Fe+2} \times (dV/dt)$. The total number of cells in the reactor (n) was estimated using the procedure described in section 2.4 and the specific iron oxidation rate was calculated from r_{Fe+2} (mol $cell^{-1}$ h^{-1}) = R_{Fe+2}/n. To estimate the cell growth rate it was assumed that entire population of cells produced planktonic daughter cells. The planktonic population count (N_p, cell L^{-1}) and dV_m/dt (L h^{-1}) were used to calculate the cell production rate R_n (cell h^{-1}) and the specific growth rate from $r_n = R_n/n$ (h^{-1}). The cell yield Y_{obs} (cell mol^{-1}), was then calculated from (R_n/R_{Fe+2})

2.4 Estimating total cell numbers in the reactor

At the chosen sampling point, cell counts were conducted to determine the planktonic population ($n_p = N_p \times V$). To estimate the total population (n) a procedure was performed on

the reactor immediately after the cell counts were taken. A known volume of the reactor fluid was withdrawn with a syringe (ca 60 mL), and then immediately returned through a filter (0.45 μm) attached to the syringe. The reduced number of cells caused an immediate reduction in the feed rate as shown in figure 2.

To estimate n it was first assumed that both planktonic and sessile cells have the same specific iron oxidation rate. This average can be expressed as equation 3 where the total iron oxidation rate in the reactor (R_{Fe+2}, mol h^{-1}) was determined using the average feed rate over 2 hours prior to the sampling point and n_s is the number of sessile cells in the reactor which together with the planktonic cells make the total number present ($n = n_p + n_s$).

$$r_{Fe+2} = R_{Fe+2}/(n_p + n_s) \qquad .3$$

Assuming an instantaneous reduction in cell numbers (C) resulting from the removal and filtration of a known fraction of the reactor volume, equation 3 can be written as two equations describing the before and after states (equations 4 and 5).

$$(R_{Fe+2})_1 = (n_p + n_s)\, r_{Fe+2} \qquad .4$$

$$(R_{Fe+2})_2 = (n_p + n_s - C)\, r_{Fe+2} \qquad .5$$

Where C is the number of cells removed during the process (N_p × volume filtered and returned), (n_p + n_s) is the total number of cells in the reactor immediately prior to the procedure. Values for $(R_{Fe+2})_1$ and $(R_{Fe+2})_2$ are expressed as a ratio R = $(R_{Fe+2})_1/(R_{Fe+2})_2$ which can be conveniently found from the ratio of the mass or volume feed rates averaged for

2 hours before (state 1) and two hours after (state 2) the medium filtration procedure. Equations 4 and 5 can be solved to yield *n*, the total number of cells in the reactor (equation 6).

$$n = -C \times R/(1 - R) \qquad .6$$

3.0 Results

3.1 Operation of the potentiostat

The continued development of a sessile population and biofilm was observed in all the experiments undertaken. Microscopic examination of swabs taken from the internal glass wall during operation showed significant numbers of cells even when there was no biofilm visible to the eye. At higher set points, E > 700 mV a white film developed rapidly, became less transparent and took on a yellow colour with further development. Microscopy of wall-swabs from this layer showed yellow solid material and cells. Wall growth *in-vitro* harbours significant numbers of cells and although a yellow film forms rapidly at higher E values, it is not necessary for significant sessile cell activity. Continuous biofilm development was exaggerated in experiments conducted at <600 mV. Over time, the sessile population n_s, protected against 'washout' by the biofilm, became large relative to the number of planktonic cells n_p and the procedure failed to give reliable estimates of the total cell numbers. Hydraulic dilution rates (D, h^{-1}) in excess of 0.48 h^{-1} were observed. Growth in all media at the higher set points E > 600 mV proved to be more stable and did not exhibit the 'run-away' biofilm development. A sessile population could be detected at higher set points but became less significant, relative to the planktonic cell population (table 4). Set points of E > 720 mV produced a relatively rapid formation of yellow solids on the internal reactor and probe

surfaces. However, within the range of 600 < E < 700 mV, continuous operation was achieved for the IEM and sulfate enriched media. The data recorded from a sequential series of steady states at increasing E values, each held for *ca* 24 hours, is shown in figure 3.

3.4 Specific rates and cell yields

Experiments observing a sequence of set points at increasing E were conducted in both IEM and IEM20 media and the derived specific parameters are given in tables 2 and 3 respectively. Data shown (Fig. 3) was used to calculate the values in table 3 (IEM20).

3.5 Switching between IEM and IEM20 media

The effect on the culture of changing the medium in the reservoir from IEM to IEM20 was examined after a period of steady state growth on IEM medium. The effect was observed as a change in the value of dM/dt (Fig. 4). The medium 'switch' did not bring about an immediate increase in TDS in the reactor because the time taken to change conditions was dependent on the dilution rate. At low E set points and high D values, the change was relatively rapid but at higher E set points and lower D values, the change required many hours: this 'medium-switch' technique was only applied to two lower E set points. The ratios $(R_{Fe+2})_{IEM}/(R_{Fe+2})_{IEM20}$ calculated at set points 604 and 644 mV were 1.8 and 1.7 respectively. The culture response to the sudden increase in TDS matched that observed when the culture was established at those same conditions *via* different paths (*cf.* tables 2 and 3).

3.6 Experiments at a range of TDS concentrations

A series of experiments at increasing Na_2SO_4 concentration were conducted, holding each steady state for more than 48 hours and sampling at least twice during the steady state. The data collect are presented in table 4 and plotted in figures 5-7.

4.0 Discussion

The continuous cultivation at fixed E values conducted in these experiments demonstrated the presence of a significant number of cells adsorbed to the reactor walls. This sessile population oxidises iron and can constitute more than half the total number of cells under certain conditions. Estimations of specific rates must consider this sessile population. An additional complication when considering iron media is that although the TDS remains constant as the iron is oxidised from Fe^{+2} to Fe^{+3}, the ionic strength *I* does not. The extra charge density of the Fe^{+3} state increases the complexation of the cation effectively reducing *I* as the solution potential increased. This change was relatively small in absolute terms ca. 0.02 - 0.03, but represented a large relative change at the minimum TDS value (Table 1). Table 2 shows that the parameter r_{Fe+2} was not constant across the E range in IEM medium. The specific rate of iron oxidation r_{Fe+2} increased as the E increased in the lowest TDS medium (IEM) but remained relatively constant in IEM20. In both media, the specific cell growth rate r_n showed an optimum between 640 and 670 mV. Two set points at 624 and 664 mV were chosen to examine the effect of TDS as the variable parameter.

4.1 The effect of increased TDS

Data from table 4 giving the specific iron oxidation rate (r_{Fe+2}) as a function of the solution TDS are plotted in Fig. 5. Values of r_{Fe+2} declined in a linear manner as the TDS was increased. There was some variation in the data for IEM and IEM10, but there was a clear

trend as the TDS increased. Operating at 70,000 ppm TDS reduced the specific iron oxidation rate to less than 25 % of that found at 30,000 ppm. Extrapolating the linear trend predicts that $r_{Fe+2} \rightarrow 0$ at a TDS value of ca 80,000 ppm however it is much more likely that iron oxidation does not cease suddenly at a particular TDS value and r_{Fe+2} continues to slow.

A plot of the specific growth rate as a function the specific iron oxidation rate is shown in Fig. 6. This relationship was also linear except for some of the highest values of r_{Fe+2} with no significant difference between experiments conducted at 624 and 664 mV. The bacterial cell reproduction rate remained directly dependent on the specific iron oxidation rate as TDS was increased. The trend in Fig. 6 shows a significant r_{Fe+2} at the point where $r_n \rightarrow 0$ indicating a 'maintenance' requirement of ca 1×10^{-14} mol cell^{-1} h^{-1} and a maximum r_n of ca 0.11 h^{-1} at both high and low set points.

The values of Y_{obs} increased as TDS increased to ca 50,000 ppm. This was followed by a significant decrease as the TDS was increased to 70,000 ppm. An optimum for Y_{obs} was evident in the region of 50,000 ppm (figure 7). While this is important for assessing autocatalytic kinetics of a process it doesn't necessarily mean that less CO_2 was reduced per mol of iron oxidised. Y_{obs} values are based on the biomass present as countable cells and don't take into account the reduced carbon present as extracellular biofilm material for example. Deriving a value for the thermodynamic yield requires an estimation of this fraction and was not included in this study.

4.2 Result interpretation

These results show that TDS, in the form of Na_2SO_4, is inhibitory to the catalysis of iron oxidation and significantly reduced the specific iron oxidation rate (r_{Fe+2}) of a heterogeneous

chemolithotrophic culture. The inhibitory effects of TDS are much less acute than those due to chloride or nitrate ions where iron oxidation is severely affected by only 5 – 7,000 ppm of chloride and lesser concentrations of nitrate (Lawson et al., 1995; Shiers et al., 2005). Increasing concentrations of Na_2SO_4 reduced r_{Fe+2} significantly but still allowed a flourishing culture, albeit at slower rates. An interpretation of the data in figure 5 can be reasonably made using the colligative properties of ionic solutions as a framework and incorporating the current models of the electron transport chain as determined for the type organism *At. ferrooxidans* (Quatrini et al., 2009). Iron oxidation requires that electrons are transferred from Fe^{+2} in the bulk solution to a cytochrome (type aa_3) in the cell membrane where oxygen is reduced to H_2O (*ibid*). The transfer takes place *via* mediators which accept the electrons and then pass them on, being reduced and then oxidised in the transfer process. The transfer steps necessarily involve a reaction between oppositely charges centres and at least the first transfer, between Fe^{+2} and the first mediator in the chain, is exposed to the colligative properties of the solution.

The colligative properties of a solution affect reaction rates by what is known as the 'kinetic salt effect' (Atkins, 1978; Longmuir, 2002) and also the 'primary salt effect' (Glasstone and Lewis, 1964). In an elementary reaction between species *x* and *y* the reaction rate is expressed as equation 7 where k , a_x and a_y are the rate constant and activities of the reacting species respectively.

$$\text{rate} = k\, a_x\, a_y \qquad .7$$

If *x* and *y* are oppositely charged, the attraction between them is reduced as the ionic strength of the medium increases making a successful reaction less likely and the effect is to reduce

the value of *k*. If *x* and *y* carry like charges then the repulsion between them is reduced as *I* increases and *k* then increases. If one or both species are uncharged, changing *I* will have no effect on *k*. At low concentrations (< 0.3 M) the magnitude of the change in *k* is a reproducible function of the square root of the change in *I*, the constant *A* from the Debye-Huckel model of ionic interactions (characteristic of the solvent and temperature $A = 1.825\times10^6\ \rho^{½}\ (\varepsilon\ T)^{-3/2}$) and the charges, z_x and z_y on the species *x* and *y* respectively (equation 8).

$$\log(k_1/k_0) = 2\ A\ z_x\ z_y\ \sqrt{(I_1-I_0)} \qquad .8$$

$$\log(r_{Fe+2\text{-}IEMi}/r_{Fe+2\text{-}IEM}) = 1.04\ z_x\ z_y\ \sqrt{I_i} \qquad .9$$

The rate constant of the rate determining step (*rds*) in the catalysed path of reaction (1) is not known but the specific iron oxidation rates r_{Fe+2} of the overall reaction can be used by assuming that the activities of *x* and *y* remain constant as *I* is varied (equation 9). The value of *A* in water at 35°C is 0.518 and equation 9 was plotted using the averaged data from table 4 yielding a linear negative slope (Fig. 8). The origin in this case is the lowest *I* value consistent with the provision of just the ionic substrates H^+ and Fe^{+2} and their associated sulfate ion.

The 'primary salt effect' model fits the inhibition observed suggesting that the rate determining step of reaction 1 is the electron transfer between Fe^{+2}(aq) and a cytochrome on the cell exterior. The value of the slope gives the product of the reacting species $z_x\ z_y = -1.57$ indicating that the *rds* in reaction 1 occurs between species of opposite charge. Assuming a cation charge of +2 gives a negative charge density of the reactive centre in the cytochrome of –0.75. The initial transfer is influenced directly by the solution *I* and the

inhibitive effect will be universal for all cells oxidising Fe^{+2} provided the *rds* and the charge density on cytochrome are unchanged. Only a limited set of conditions has been tested here but the primary salt effect at least provides a falsifiable hypothesis for the effect of increasing TDS and *I*. Other effects of a change in the medium *I*, such as an increased osmotic gradient across the cell membrane and changes in the relative activities of Fe^{+2} and $FeSO_4°$, have yet to be examined and reported.

4.3 Industrial Implications

The oxidation of Fe^{+2} in acidic solution is an important step in a wide variety of hydrometallurgical processes. Bacterial catalysis represents a control tool, capable of rapidly converting Fe^{+2} to Fe^{+3} from the input of just atmospheric oxygen. These results are pertinent because all leachate streams contain TDS leached from the gangue content of the target mineral and elevated concentrations exert a significant inhibitory effect on the rate of oxidation that a cell can achieve. The simple relationship in figure 5 shows that the Fe^{+3} production rate can be doubled by reducing the TDS from 70,000 to 50,000 ppm. It's proposed that the inhibition by TDS arises from the change in solution properties and will therefore affect any iron oxidising organisms to similar extents. These data can not be extrapolated beyond 0.4 M because the assumptions implicit in equation 8 become increasingly strained.

The nature of the ions making up the TDS fraction will vary with the nature of the mineral being processed and the common anions Cl^- and NO_3^- demonstrate toxic rather than inhibitory effects at concentrations of ~5,000 ppm. However the observed effects of sulfate and the common cation constituents Na^+, K^+, NH_4^+ and Al^{+3} suggest that only the cation's contribution to the colligative properties of the medium is important (Blight and Ralph, 2004; Blight and Ralph, 2008a). Whether the presence of the target metal cations, usually the divalent Cu^{+2}, Zn^{+2}, Ni^{+2} and Co^{+2} have effects beside their contribution to *I* is not known but adaptation to varying concentrations is reported (Watling, 2006). Reducing TDS values in a process circuit is not a simple matter but these results can give some reliability to estimates of the cost of operating at elevated TDS concentrations.

5.0 Conclusions

Control over the speciation of iron in acid solution, in particular its oxidation to Fe^{+3}, can be achieved by the growth of aerobic chemolithotrophic bacteria. This study demonstrates the inhibitory effects of the TDS fraction that accumulates in hydrometallurgical processes. The specific substrate oxidation rate (r_{Fe+2}, mol $cell^{-1}$ h^{-1}) of an iron oxidising culture was reduced when sodium sulfate was added. Increasing the TDS to 70,000 ppm reduced r_{Fe+2}, to ca 25 % of that found at low TDS (< 20,000 ppm). The magnitude of the inhibitive effect of TDS can be explained by the colligative properties of aqueous solutions. A reduction in TDS will enhance the rate of iron oxidation and these results give some reliability to estimations of the improvement expected from a particular reduction in TDS. A comparison of the costs of TDS reduction with the benefits of faster Fe^{+3} production and greater productivity also becomes more reliable.

Acknowledgements

Support from the A.J. Parker Cooperative Research Centre for Integrated Hydrometallurgy Solutions and Murdoch University are acknowledged. The technical assistance of Mr. John Cronin in determining the vapour pressure above iron solutions is also acknowledged.

References

Alexander, B., Leach, S., Ingledew, W.J., 1987. The relationship between chemiosmotic parameters and sensitivity to anions and organic acids in the acidophile *Thiobacillus ferrooxidans*. J. Gen. Microbiol., 133, 1171-1179.

Atkins P.W., 1978. Physical Chemistry. Oxford University Press.

Blight, K.R., Ralph, D.E., 2004. Effect of ionic strength on iron oxidation with batch cultures of chemolithotrophic bacteria. Hydrometallurgy 73, 325–334.

Blight, K.R., Ralph, D.E., 2008. Aluminium sulphate and potassium nitrate effects on batch culture of iron oxidising bacteria. Hydrometallurgy 92, 130–134.

Bridge, T.A.M., Johnson, D.B., 1988. Reduction of soluble iron and reductive dissolution of ferric iron minerals by moderately thermophilic iron oxidising bacteria. Appl. Microbiol. Biotechnol. 51, 820-826.

Bridge, T.A.M., Johnson, D.B., 2000. Reductive dissolution of ferric iron minerals by *Acidiphilium* SJH. Geomicrobiol. J. 17, 193-206.

Brock, T.D., Gustafson, J., 1976. Ferric iron reduction by sulphur- and iron-oxidising bacteria. Appl. Environ. Microbiol. 32(4), 567-571.

Burkin, A.R., 2001. Chemical hydrometallurgy. Imperial college Press.

Candy, R.M., Blight, K.R., Ralph, D.E. 2009. Specific iron oxidation and cell growth rates of bacteria in batch culture. Hydrometallurgy 98, 148–155.

du Plessis, C.A., Slabbert, W., Hallberg, K.B., Johnson, D.B., 2011. Ferredox: A biohydrometallurgical processing concept for limonitic nickel laterites. Hydrometallurgy 109, 221-229,

Gahan, CS., Sundkvist J-E., Dopson, M and Sandstrom A., 2010. Effect of chloride on ferrous iron oxidation by a *Leptospirillum ferriphilum*-dominated chemostat culture. Biotechnology and Bioengineering 106, 422 - 431.

Glasstone, S., Lewis, D., 1964. Elements of physical chemistry. McMillan. London.

Hallberg, K., Grail, B.M., du Plessis, C.A., Johnson, D.B., 2011. Reductive dissolution of ferric iron minerals: a new approach for bioprocessing nickel laterites. Miner. Eng. 24, 620-624.

Kazadi, T.K., Petersen, J., 2008. Kinetic measurement of biological oxidation of ferrous iron at low ferric to ferrous ratios in a controlled potential batch reactor. Hydrometallurgy 94 (1–4), 48–53.

Lawson, E.N., Nicholas, C.J., Pellat, H., 1995. The toxic effects of chloride ions on thiobacillus ferrooxidans. In Biohydrometallurgy Processing, Vargas, T., Jerez, C.A., Wiertz, J.V., Toledo, H. (Eds.). University of Chile.

Lowson, R. 1982. Aqueous oxidation of pyrite by molecular oxygen. Chemical Reviews, 82, 461-497.

Langmuir, D., 1997. Aqueous environmental geochemistry. Prentice-Hall.

Meruane, G., Salhe, C., Wiertz, J., Vargas, T., 2002. Novel electrochemical-enzymatic model which quantifies the effect of the solution Eh on the kinetics of ferrous iron

oxidation with *Acidithiobacillus ferrooxidans*. Biotechnology and Bioengineering 80 (3), 280–288.

Nemati, M., Harrison, S.T.L., Hansford, G.S., Webb, C., 1998. Biological oxidation of ferrous sulfate by *Thiobacillus ferrooxidans*: a review on the kinetic aspects. Biochemical Engineering Journal 1 (3), 171–190.

Ojumu, T.V., Petersen, J., Searby, G.E., Hansford, G.S., 2006. A review of rate equations proposed for microbial ferrous-iron oxidation with a view to application to heap bioleaching. Hydrometallurgy 83 (1–4), 21–28.

Quatrini, R., Appia-Ayme, C., Denis, Y., Jedlicki, E., Holmes, DS., Bonnefoy, Y. 2009. Extending the models for iron and sulfur oxidation in the extreme acidophile *Acidithiobacillus ferrooxidans*. BMC Genomics 10:394.

Shiers, D.W., Blight, K.R., Ralph, D.E., 2005. Sodium sulfate and sodium chloride effects on batch culture of iron-oxidizing bacteria. Hydrometallurgy 80 (1–2), 75–82.

Sundkvist, J-E., Gahan, C.S., Sandström, Å., 2007. Modeling of ferrous iron oxidation by a *Leptospirillum ferrooxidans*-dominated chemostat culture. Biotechnology Bioengineering 99 (2), 378–389.

Watling, H.R., 2006. The bioleaching of sulphide minerals with emphasis on copper sulphides – A review. Hydrometallurgy 84 (2006) 81–108.

Table 1

TDS and ionic strength values of the media used in this study. I_{500} and I_{700} refer to the values with the iron present as the Fe^{+2} and Fe^{+3} states respectively.

Table 2

Specific cell parameters at five steady states in IEM medium.

Table 3

Specific cell parameters at six steady states in IEM20 medium (raw data from figure 3).

Table 4

Specific cell parameters derived from steady states at increasing TDS.

Table 1

TDS and ionic strength values of the media used in this study. I_{500} and I_{700} refer to the values with the iron present as the Fe^{+2} and Fe^{+3} states respectively.

Medium	TDS/ppm	I_{500}	I_{700}
IEM	12 000	0.066	0.043
IEM10	22 000	0.121	0.098
IEM20	32 000	0.180	0.156
IEM40	52 000	0.289	0.265
IEM60	72 000	0.382	0.360

Table 2

Specific cell parameters at five steady states in IEM medium.

Medium	**IEM**				
Set point (mV)	**584**	**614**	**644**	**674**	**704**
r_{Fe+2} (mol cell^{-1} h^{-1})/10^{-14}	7.5	8.4	7.5	9.3	10.9
r_n (h^{-1})	0.043	0.065	0.070	0.083	0.067
Y_{obs} (cell mol^{-1})/10^{11}	5.7	7.7	9.2	8.9	6.3

Table 3

Specific cell parameters at six steady states in IEM20 medium (raw data from figure 3).

Medium	**IEM20**					
Set point (mV)	**604**	**624**	**644**	**664**	**684**	**704**
r_{Fe+2} (mol cell^{-1} h^{-1})/10^{-14}	4.5	5.1	6.0	7.1	6.6	6.3
r_n (h^{-1})	0.042	0.051	0.058	0.056	0.047	0.030
Y_{obs} (cell mol^{-1})/10^{11}	9.3	10	9.7	7.9	7.1	4.8

Table 4

Specific cell parameters derived from steady states at increasing TDS.

Medium	set point /mV	Sampling time (h)	Planktonic cell fraction n_p/n	r_{Fe+2} (mol cell^{-1} h^{-1}) /10^{-14}	r_n (h^{-1})	Y_{obs} (cell mol^{-1}) /10^{11}
IEM00	624	19	0.63	9.2	0.071	7.8
		72	0.87	15.0	0.117	7.8
	664	25	0.86	16.1	0.112	7.0
		49	0.74	17.5	0.106	6.0
IEM10	624	21	0.60	10.3	0.071	6.9
		44	0.69	11.4	0.087	7.6
	664	24	0.59	8.7	0.081	9.3
		45	0.40	6.9	0.053	7.6
IEM20	624	23	0.99	12.1	0.110	9.1
		46	0.81	9.5	0.090	9.6
	664	22	0.86	8.5	0.087	10.2
		47	0.86	7.9	0.081	10.3
IEM40	624	18	0.86	8.1	0.062	7.6
		42	0.60	5.1	0.042	8.3
	664	20	0.73	4.1	0.047	11.3
		46	0.99	7.0	0.072	10.2
		68	0.90	5.9	0.057	9.6
		93	0.92	6.9	0.059	8.6
IEM60	624	21	1.0	2.8	0.043	4.3
		47	0.30	2.8	0.010	3.4
	664	32	0.52	1.4	0.008	5.3
		55	0.62	2.1	0.008	4.1

Fig.1. Data recording of reservoir mass (■) and solution potential (□) during steady state operation at a set point of 624 mV in IEM20 medium.

Fig. 2. Solution potential (□) and reservoir mass before (■) and after (●) removal, filtration and return of 44 % of the reactor fluid during a steady state at 674 mV in IEM medium.

Fig. 3. Solution potential (solid line) and reservoir mass (dotted line) data generated at a series of set points in IEM20 medium. Note the change in medium reservoir at *ca* 90 hours.

Fig. 4. Solution potential (□) and reservoir mass during a switch from IEM (■) to IEM20 (●) medium during a steady state at 604 mV. Medium mass addition rates (dM/dt) for IEM and IEM20 were 139 and 69.8 g h^{-1} respectively.

Fig. 5. The specific iron oxidation rates as a function of TDS at E = 624 (♦) and E = 664 (□) mV.

Fig. 6. The specific cell growth rate (r_n) as a function of the specific iron oxidation rate (r_{Fe+2}) at E = 624 (♦) and E = 664 (□) mV in all media.

Fig. 7. The cell yield (Y_{obs}) as a function of TDS at E = 624 (♦) and E = 664 (□) mV.

Fig. 8. Data from tables 1 and 4 interpreted using the 'Primary salt effect' model. Slope of the fitted line was m = -1.57 and R^2 = 0.992.

Fig.1. Data recording of reservoir mass (■) and solution potential (□) during steady state operation at a set point of 624 mV in IEM20 medium.

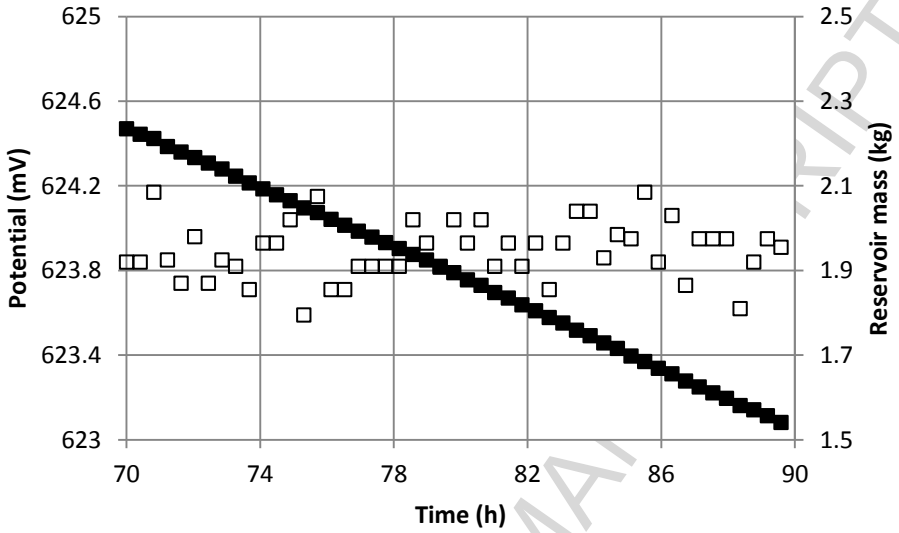

Fig. 2. Solution potential (□) and reservoir mass before (■) and after (●) removal, filtration and return of 44 % of the reactor fluid during a steady state at 674 mV in IEM medium.

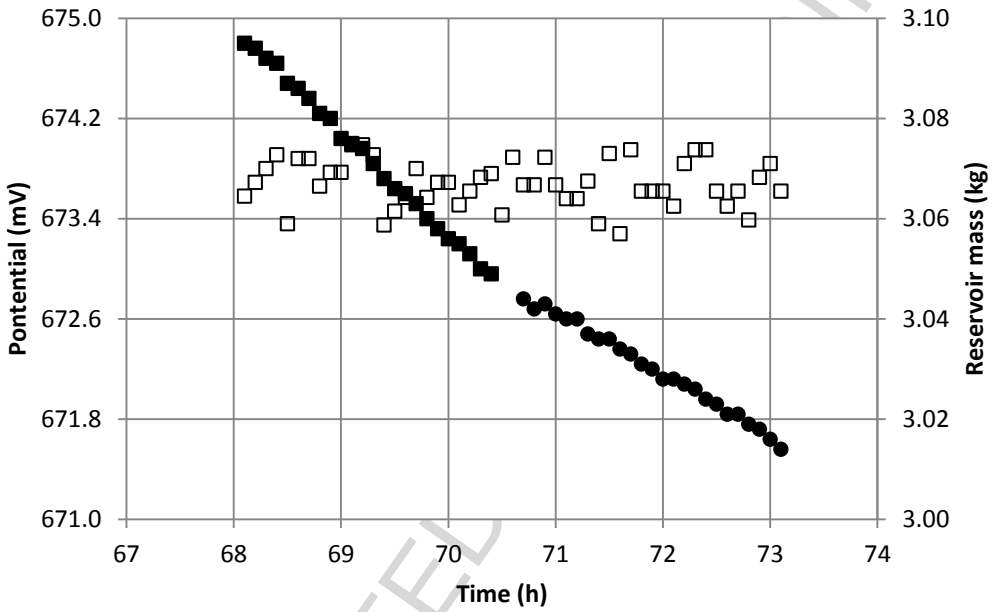

Fig. 3. Solution potential (solid line) and reservoir mass (dotted line) data generated at a series of set points in IEM20 medium. Note the change in medium reservoir at *ca* 90 hours.

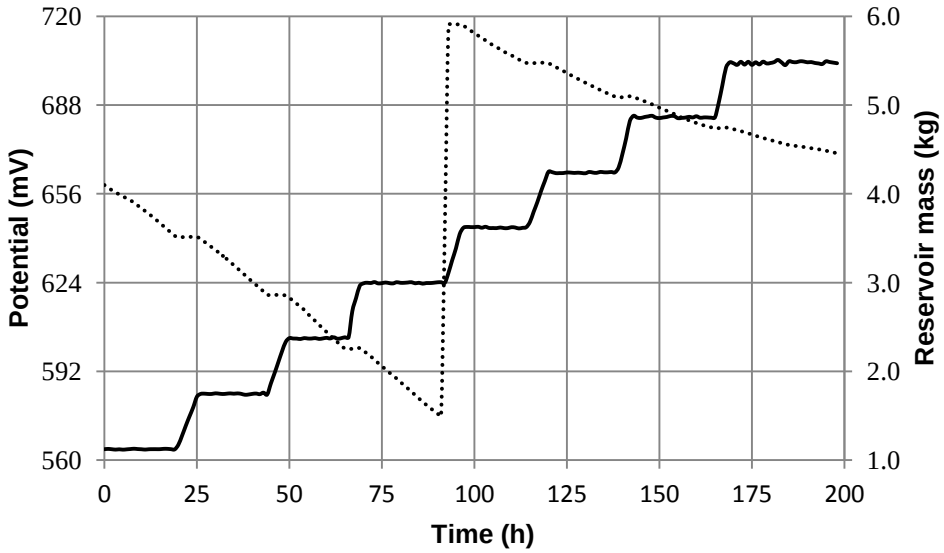

Fig. 4. Solution potential (□) and reservoir mass during a switch from IEM (■) to IEM20 (●) medium during a steady state at 604 mV. Medium mass addition rates (dM/dt) for IEM and IEM20 were 139 and 69.8 g h^{-1} respectively.

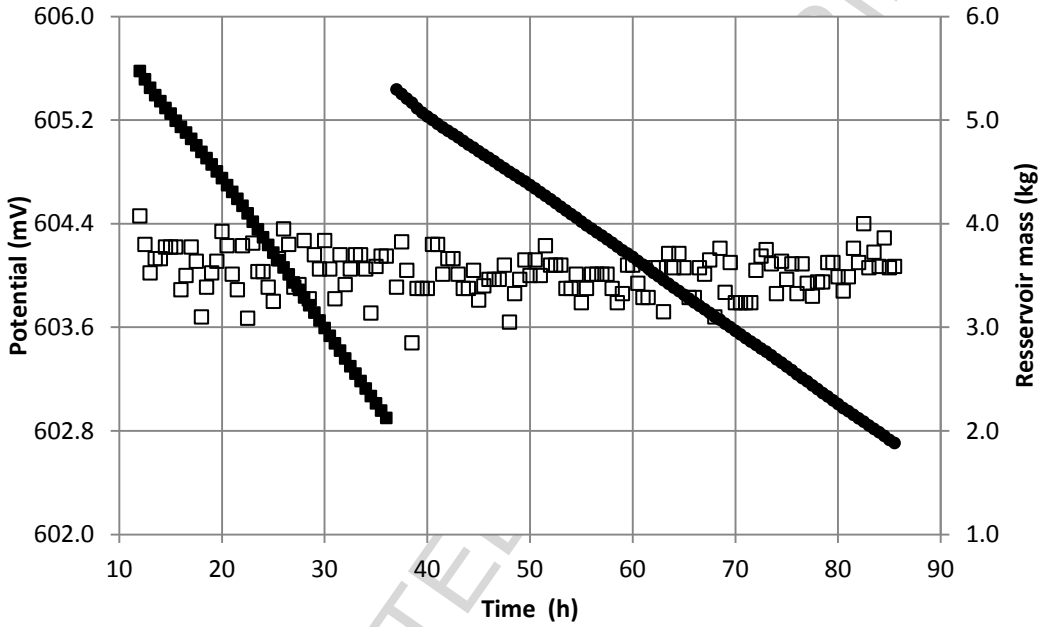

Fig. 5. The specific iron oxidation rates as a function of TDS at E = 624 (♦) and E = 664 (□) mV.

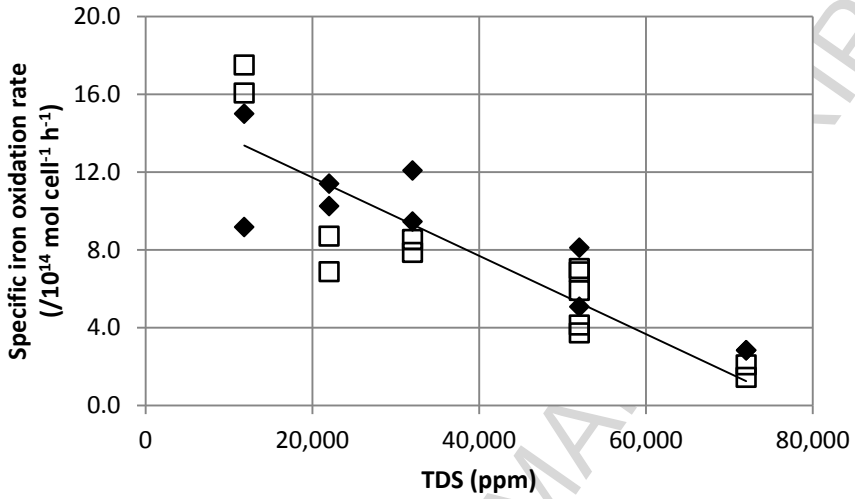

Fig. 6. The specific cell growth rate (r_n) as a function of the specific iron oxidation rate (r_{Fe+2}) at E = 624 (♦) and E = 664 (□) mV in all media.

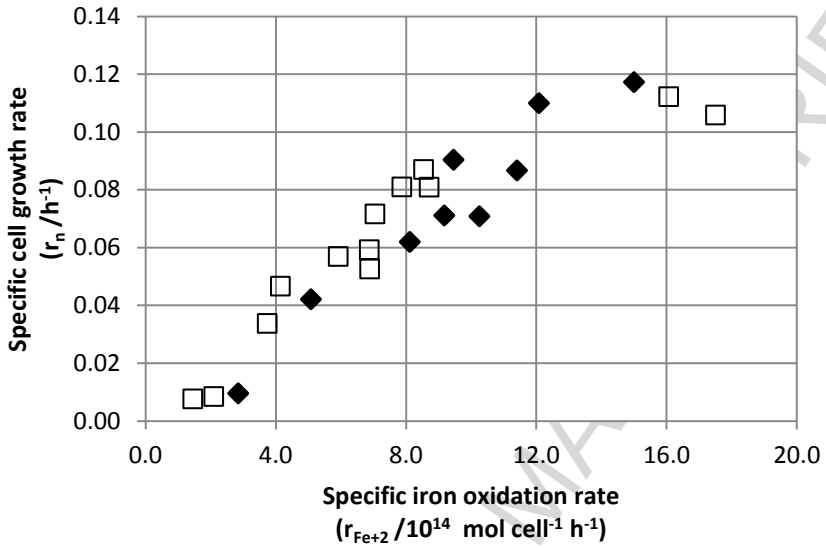

Fig. 7. The cell yield (Y_{obs}) as a function of TDS at E = 624 (♦) and E = 664 (□) mV.

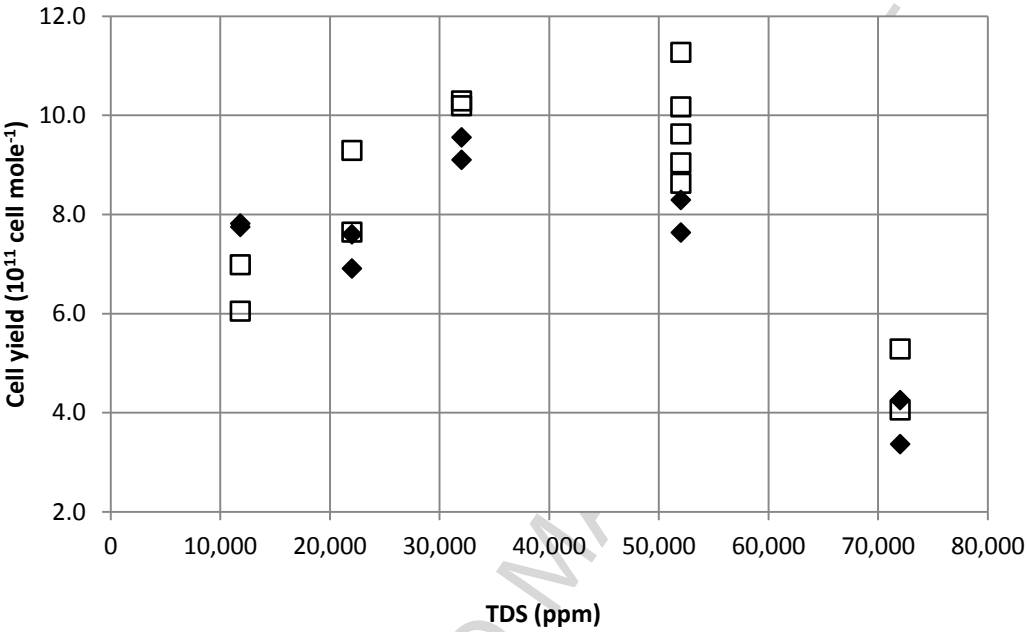

Fig. 8. Data from tables 1 and 4 interpreted using the 'Primary salt effect' model. Slope of the fitted line was m = -1.57 and R^2 = 0.992.

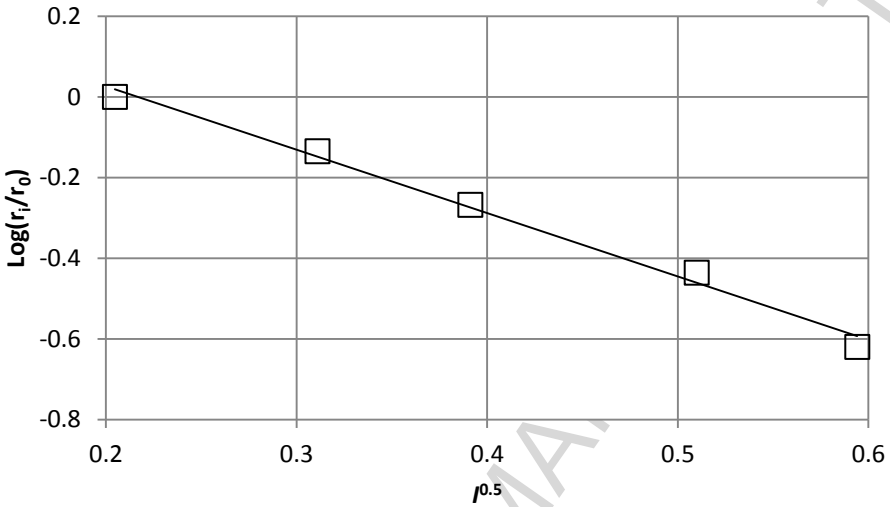

Highlights

Total Dissolved Solids and their Effects on Iron oxidation by Chemolithotrophic Cells

K.R. Blight, R.M. Candy, M.J.M. Menzel and D.E. Ralph

A.J. Parker Cooperative Research Centre for Integrated Hydrometallurgy Solutions, School of Chemical and Mathematical Sciences, Murdoch University, South Street, Murdoch, Western Australia 6150, Australia.

Colligative properties of the medium in which cells grow can exert significant influences on the rate of metabolic processes within the cell. We have shown that these effects can influence and quantitatively proscribe the rate of iron oxidation by these chemolithotrophic cells. The highlight of this research is the direct connection between the behaviour of the culture under examination and the physical or colligative properties of the solution.